

Methodology for the Analysis of ASTM A335 P92 Steel Exposed to Real Atmospheres of Refinery Combustion

Juan Orozco^{a,*}, Viatcheslav Kafarov^a, Dario Peña^b

^aUniversidad Industrial de Santander, Escuela de Ingeniería Química, Centro de Investigación para el Desarrollo Sostenible en Industria y Energía – CIDES, Cra 27 calle 9, Bucaramanga -Santander (Colombia).

^bUniversidad Industrial de Santander, Escuela de Ingeniería Metalúrgica y Ciencia de Materiales, Grupo de Investigaciones en Corrosión – GIC, Cra 27 calle 9, Bucaramanga -Santander (Colombia).
juan.orozco1@correo.uis.edu.co / ingjorozcoa@gmail.com

This work proposes a methodology for the study of the physical and chemical effects of the materials used in the petrochemical industry, specifically ASTM A335 P92 steel. This methodology includes stages such as: selection of atmospheres and determining variables, experiment design, preliminary tests and experiment calibrations, manufacture of corrosion coupons, experimentation of the material with the different environments, kinetic study, characterization of the material by means metallographic analysis, of hardness and micro-hardness, scanning electron microscopy (SEM), energy-dispersive X-ray spectroscopy (EDS), X-ray diffraction analysis (XRD), X-ray photoelectron spectroscopy (XPS) and finally discussion of results. This paper studies four corrosion phenomena at high temperatures: oxidation, nitridation, carburization and water vapor effect. Within the working conditions, five exposure times (1, 20, 50, 100 and 200 h) and four service temperatures (450, 550, 650 and 750 °C) were selected.

1. Introduction

The permanent need that involves maintaining and improving efficiency in production processes at the industry promotes the use of high temperatures, which advantage the presence of more severe corrosive environments on the materials with which the different equipment works. In an industrial complex more than 70 % of the materials are metals and depending on the characteristics and uses of this location most of the metals used are carbon steels, that is, they are ferrous materials of low alloy and very susceptible to corrosion attack due to the interaction with the different predominant atmospheres (Casallas, 2011). For the year 2015, the approximate annual direct cost of corrosion for the United States was estimated at USD 500,000 million, which represents about 3.1 % of the gross domestic product (GDP) of that country (Asrar et al., 2016). Likewise, it is estimated that industrialized countries spend around 5 % of their gross domestic product in preventing and correcting problems related to corrosion. To counteract this situation, materials such as ferritic steels have been developed, which are a series of alloys that advantage the increase of the life of the metallic components of the equipment, further being able to operate each time at higher temperatures to achieve greater efficiency in the conversion of raw materials, which translates into greater profitability in the processes (Peña et al., 2012). ASTM A335 P92 steel is widely used in processes that require operating at high temperatures according to Peña et al. (2014) due to the addition of elements such as W, Nb, V and Mo. This alloy is of great use in equipment to transport steam at high temperatures, mainly due to its good resistance to creep and corrosion reported by Gamo (2016).

The phenomena of oxidation, carburization, nitridation and the effect of water vapor are four of the most important corrosive phenomena that occur in combustion environments at high temperatures. It is believed that one of the main reasons why steels with 9 % chromium have such high corrosion rates in the presence of combustion gases, is due to the presence of water vapour (Galerie et al., 2011). Oxidation is the most influential and important surface reaction at high temperatures. Many industrial environments have sufficient oxygen activity to allow this reaction. In the petrochemical industry, carburization is one of the main corrosive phenomena that occur in processes at high temperatures, mainly due to the formation of internal carbides,

which often cause the materials to suffer fragility (Young, 2016). The nitridation phenomenon occurs when the oxide layers do not provide a protective character on the alloy. Above nitriding the factor that controls the process is nitrogen activity (Pettit, 2011).

This research is part of the set of studies where the combustion process was studied by simulation tools and experimentally, in this work was used software PREMIX for evaluate combustion of representatives mixtures of refining industry; the simulation model used described an isobaric system, in steady state and unidirectional, and reaction mechanics is carried out using GRI-MECH 3.0 this results obtained by simulation and experimentally show agreement with data reported in the literature for combustion products, temperature and propagation flame rate (Kafarov et al., 2015), the behaviors of the AISI 304 and ASTM A335 P5 steels exposed to combustion atmospheres were evaluated. The corrosion products formed on each material were simulated at 750 °C in the HSC Chemistry software, where the SEM-EDS analysis showed that the corrosion products formed on AISI 304 steel corresponded mainly to iron oxides and spinels (Alviz et al., 2017) and the effects of interchangeability and energy efficiency in the petrochemical industry were studied. Statistical analysis was developed in combustible gases to study their composition considering the origin of each of the streams represented by chromatographic analysis, which, provided the data for calculating the methane's number (MN) via method radius ratio (H/C), and the Wobbe index as criteria for analysing the potential effect of gas fuel composition in efficiency, integrity and environmental emissions equipment (Saavedra et al., 2014).

2. Methodology

In order to fulfill the objectives proposed in this work, a set of methods was established (see Figure 1).

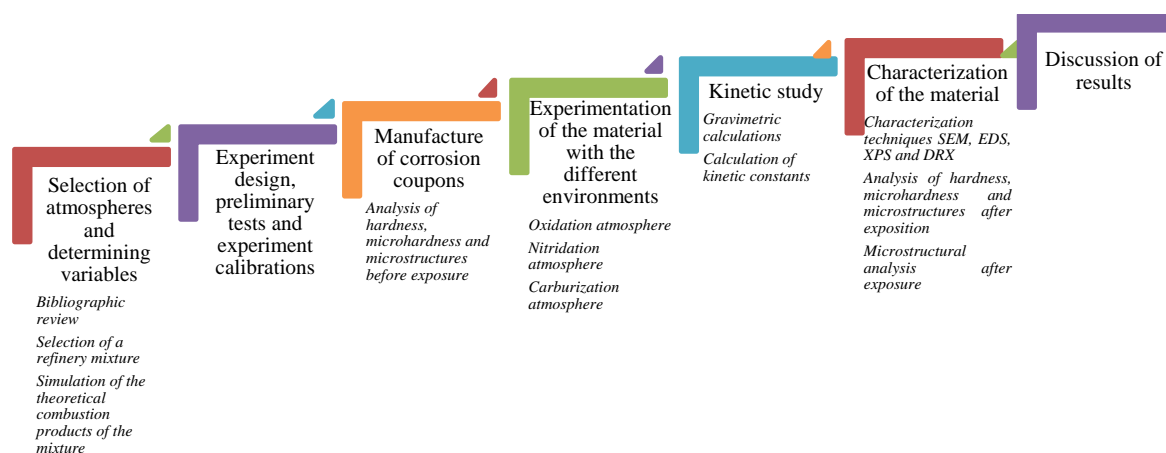


Figure 1. Methodology proposed for the corrosive study of materials used in the petrochemical industry

2.1 Selection of atmospheres and determining variables

Initially, a bibliographic review was carried out with the objective of determining the values of the variables, such as: mass flow, temperatures, exposure times and pressure. Likewise, a characteristic mixture of refinery gases was obtained (Cala et al., 2013). Finally, the simulation of the combustion process of this mixture was carried out with an excess of air of 10 % in the simulation software Aspen Hysys.

2.2 Experiment design, preliminary tests and experiment calibrations

Considering the composition of each atmosphere to be evaluated and the variables selected, proceeded to carry out the experimental assembly, calibration of equipment and preliminary tests.

2.3 Manufacture of corrosion coupons

The material cutting process was carried out until obtaining a rectangular parallelepiped shape with dimensions of 15 mm x 10 mm x 2 mm. The preparation of the coupons was accomplished following the standard ASTM G1-03 "Standard Practice for Preparing, Cleaning, and Evaluating Corrosion Test Specimens".

2.4 Experimentation of the material with the different environments

At this stage, the exposure of the material to each of the study atmospheres (oxidation-water vapor, oxidation-nitridation-water vapor and oxidation-carburization-water vapor) was carried out.

2.5 Kinetic study

The kinetic study was carried out by gravimetric calculations to determine the gain or loss of mass in the material as a function of time, to analyze the kinetic behavior and to know the kinetic constants of the speed laws described.

2.6 Characterization of the material

The material was characterized by means of physical, chemical and mechanical analysis, through the techniques of Energy Dispersive X-ray Spectroscopy (EDS), Scanning Electron Microscopy (SEM), X-ray Diffraction (XRD) and X-ray Photoelectron Spectroscopy (XPS).

2.7 Discussion of results

Finally, all the results obtained in the study were analyzed.

3. Results

According to the simulation carried out in stage number 1 of the proposed methodology, three study mixtures were determined.

3.1 Calculation of the composition of the study mixtures

Initially, the composition of the study mixtures was determined, this results can be observed in Table 1, Table 2 and Table 3. Also, the composition of ASTM 3353 P92 steel is presented in Table 4.

Table 1: Oxidation-water vapor mixture composition

Compounds	O ₂	H ₂ O
% Molar	9.5	90.5

Table 2: Oxidation-nitridation-water vapor mixture composition

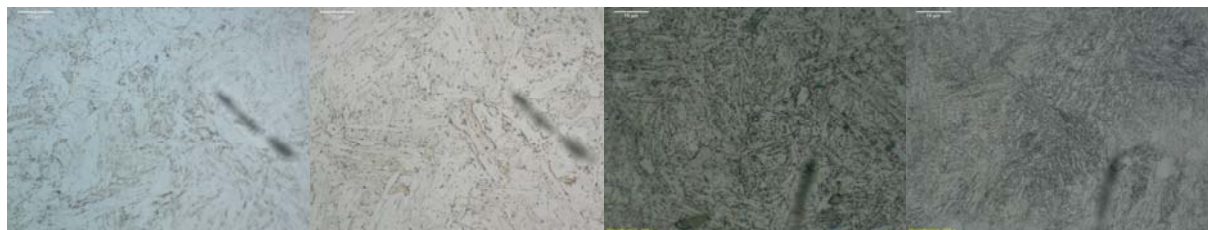
Compounds	O ₂	H ₂ O	N ₂
% Molar	1.9	18.4	79.7

Table 3: Oxidation-carburization-water vapor mixture composition

Compounds	O ₂	H ₂ O	CO ₂
% Molar	6.3	60.6	33.1

Table 4. Composición en peso del acero ASTM A335 P92

Element	C	Mn	Si	P	S	Cr	Mo
% weight	0.115	0.454	0.220	0.013	0.0033	9.14	0.4
Element	Ni	Al	V	Nb	W	N	B
% weight	0.119	0.011	0.165	0.055	1.979	0.039	0.022



a)

b)

c)

d)

Figure 2: Optical microstructure of steel ASTM A335 P92 (500x) a) Initial state without exposure to combustion atmospheres; b) microstructure oxidation-nitridation - water vapor after 200 h of exposure and temperature of 750 °C; c) microstructure oxidation-water vapor after 200 h of exposure and temperature of 750 °C; d) microstructure oxidation-carburization-water vapor after 200 h of exposure and temperature of 750 °C

Figure 2a shows the microstructure of the steel before being exposed to combustion atmospheres, it is possible to observe a ferrite matrix with martensitic structure due to the amount of chromium in ASTM A335 P92 steel;

Figure 2b shows a microstructure similar to observed in Figure 2a, however, it is evident the presence of carbides and carbonitrides that dissolve and precipitate at the edges due to the content of alloying elements such as molybdenum, vanadium, iron, chrome, among others; in Figure 2c a greater precipitation of the formed carbides is observed, also a obscuration in the microstructure can be observed due to the effect of the high temperatures; finally, in Figure 2c, it is possible observe more needles formed in the material, which is due to the formation of carbides in large proportion given the greater carbon activity mainly due to the composition of the study atmosphere evaluated.

3.2 Scanning Electron Microscopy (SEM)

Figure 3a shows the formation of 3 surface layers, which have good homogeneity between them, also, it can be seen that the chromium rich inner layer is a layer with good protective behavior, the average thickness of these three layers is 315.9 μm ; Figure 3b shows the formation of 2 layers, which have porosity, mainly due to cracks in the upper layer, these two layers do not have a good adhesion, the average thickness of these 2 layers was 150.9 μm ; finally in Figure 3c is observed the formation of layers with low homogeneity, the upper layer has cracks and macro-cracks due to internal stresses developed on the surface by prolonged exposure and high temperatures, the average thickness of these 2 layers is 110.2 μm .

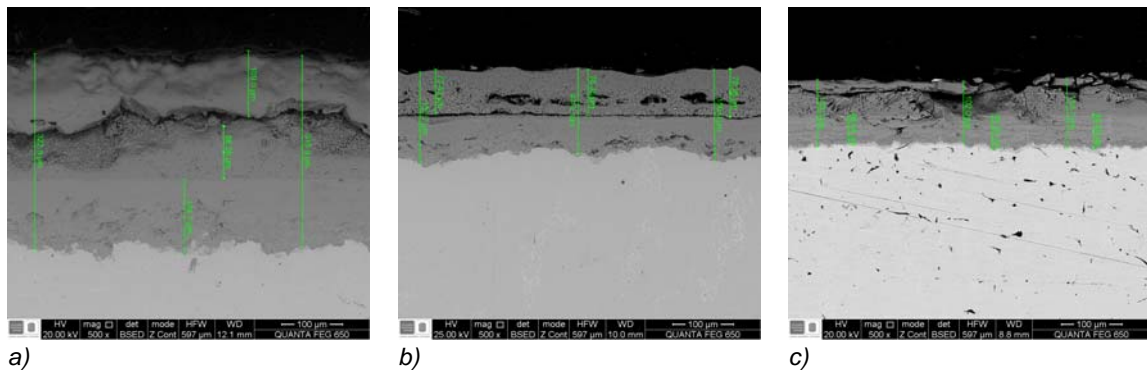


Figure 3: Scanning electron microscopy (SEM) of ASTM A335 P92 steel (500x) a) Oxidation-water vapor after 200 h of exposure and temperature of 750 °C b) Oxidation-nitridation-water vapor after 200 h of exposure and temperature of 750 °C c) oxidation-carburization-water vapor after 200 h of exposure and temperature of 750 C

3.3 Kinetic study

Due to the protective nature of the inner layer observed in Figures 2a, 2b and 2c, the chemical kinetics of the studied environments is controlled by the diffusion of the ions. The exposure time vs. mass gain graphs for Figures 3a, 3b and 3c have a parabolic character. At temperatures greater than 500 °C, the growth rate of a thickness layer "x" is controlled by diffusion and can usually be described by equation 1 (Gamo, 2016):

$$x_t^2 - x_{t_0}^2 = 2 * k(t - t_0) \quad (1)$$

Where k is the velocity constant, x is the thickness of the layer and t is the time.

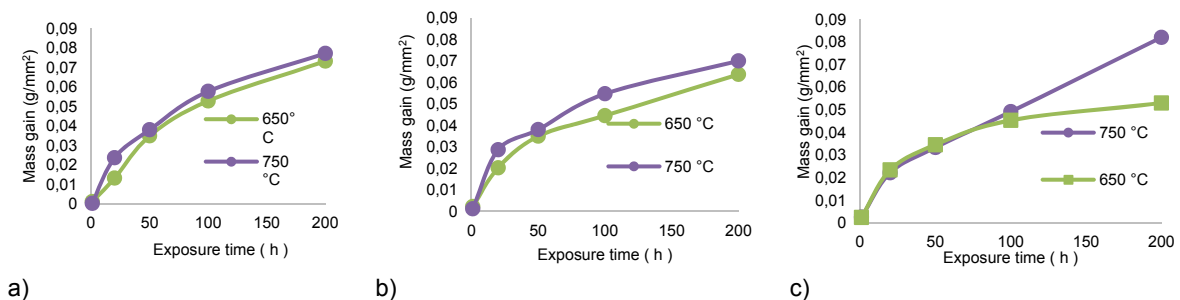


Figure 4: Exposure time vs mass gain a) Oxidation-water vapor environment b) Oxidation-nitridation-water vapor environment c) Oxidation-carburization-water vapor environment

The chemical kinetics for ASTM A335 P92 steel in the study environments is presented in Table 5, Table 6 and Table 7.

Table 5: Chemical kinetics of ASTM A335 P92 steel for the oxidation-water vapor environment at 650 °C and 750 °C

Temperature (°C)	Kinetics Law	Error
650	$2.79 \times 10^{-5}t - 1.50 \times 10^{-4}$	1.70×10^{-4}
750	$3.03 \times 10^{-5}t + 1.2 \times 10^{-5}$	1.90×10^{-4}

Table 6: Chemical kinetics of ASTM A335 P92 steel for the oxidation-nitridation-water vapor environment at 650 °C and 750 °C

Temperature (°C)	Kinetics Law	Error
650	$2.01 \times 10^{-5}t + 5.00 \times 10^{-5}$	1.10×10^{-4}
750	$2.43 \times 10^{-5}t + 2 \times 10^{-4}$	2.70×10^{-4}

Table 7: Chemical kinetics of ASTM A335 P92 steel for the oxidation-carburization-water vapor environment at 650 °C and 750 °C

Temperature (°C)	Kinetics Law	Error
650	$2.01 \times 10^{-5}t + 5 \times 10^{-5}$	1.10×10^{-4}
750	$3 \times 10^{-5}t + 2 \times 10^{-4}$	2.70×10^{-4}

3.4 Energy Dispersive X-ray Spectroscopy (EDS)

Through the analysis of (EDS) for the working temperatures 450, 550, 650 and 750 °C and considering 3 study environments, it was observed that the highest atomic and mass percentage in the external, intermediate and internal layers corresponded in first place the element iron (Fe), then the oxygen (O). For the chromium (Cr) it was possible to appreciate that it is atomic and mass percentage was greater for the internal layers.

3.5 X-ray Diffraction (XRD)

Through the X-ray Diffraction (XRD) analysis, the corrosion products were determined in the material. These results are presented in Table 8.

Table 8: Products formed in the material analyzed through the XRD technique

Products	Name	Temperature (°C)	Exposure time (h)	Environment
Fe ₂ O ₃	Hematite	750-650	200-100-50-20	oxidation, nitridation, carburization
Fe ₃ O ₄	Magnetite	750-650	200-20	oxidation, nitridation, carburization
F ₃ N _{1.1}	Iron nitride	750	200-20	oxidation, nitridation
Fe(OH) ₃	Iron (III) oxide-hydroxide	650	50	oxidation, nitridation
Fe(Cr ₂ O ₄)	Chromite	750	200	oxidation, nitridation,

3.6 X-ray Photoelectron Spectroscopy (XPS)

Table 9 shows the results obtained by means of the X-ray Photoelectron Spectroscopy (XPS) analysis.

Table 9: Products formed in the material analyzed through the XPS technique

Products	Name	Temperature (°C)	Exposure time (h)	Environment
Fe ₂ O ₃	Hematite	750-650	200-100-50-20	oxidation, nitridation, carburization
Fe ₃ O ₄	Magnetite	750-650	200-20	oxidation, nitridation, carburization
FeO	Wustite	450-550	200-20	oxidation, nitridation
Si ₃ N ₄	Silicon Nitride	650-750	50	nitridation
NSiO ₂	Silicon oxynitride	750	200	nitridation
Cr ₃ C ₂	Chromium carbide	650	200	carburization

3.7 Analysis of hardness and microhardness

Hardness and microhardness in the initial state of the ASTM A335 P92 steel was 60.2 HRA and 310.9 HV respectively, for the study environments at temperatures of 450, 550 and 650 °C and exposure times of 1, 20, 50, 100 and 200 h, the steel did not show significant changes, mainly because the maximum working temperature of this material is in the temperature range between 610 - 640 °C. For the temperature of 750 °C there was a considerable decrease, with values of hardness in the range of 50 - 52 HRA, as well as microhardness values between 260 - 280 HV, mainly due to the increase of the diffusive processes.

4. Conclusions

In present work the methodology for the analysis of materials used in the petrochemical industry exposed to real atmospheres of refinery combustion was proposed and applied to ASTM A335 P92 steel. Considering the analyzes accomplished on steel exposed to atmospheres of oxidation, nitridation, carburization and water vapor, it was observed that this material presented a good behavior for the temperatures of 450, 550 and 650 °C for the exposure times of 1, 20, 50, 100 and 200 h, however, at the temperature of 750 °C defects were observed in the morphology (cracks and macro-cracks) as well as decreases in hardness and microhardness, which can lead to equipment failure, mainly due to exceeding the maximum working temperature of the material.

The kinetic behaviors obtained for the working temperatures of 650 and 750 °C at the different exposure times were parabolic, characteristic behavior of diffusion-controlled processes.

Acknowledgments

The authors expressed their acknowledgments to the Administrative Department of Science, Technology and Innovation of Colombia (COLCIENCIAS) and Colombian Network of Knowledge in Energy Efficiency (RECIEE) for financial support of this work that is part of the project "Consolidation of the knowledge network on energy efficiency and its impact on the productive sector under international standards - Design of a methodology for the eco-efficient management of combustion processes, case study: the oil refining industry" code of COLCIENCIAS: 110154332086 and Grupo de Investigaciones en corrosión (GIC).

References

- Alviz A., Kafarov V., Meriño L., 2017, Methodology for evaluation of corrosion damage during combustion process in refinery and petrochemical industry. Case study: AISI 304 and ASTM A335 P5 steels, *Chemical Engineering Transactions*, 61, 1315–1320.
- ASTM Standard G1-03, 2011, Standard practice for preparing, cleaning, and evaluating corrosion test specimens, ASTM International, West Conshohocken, PA.
- Cala O.M., Meriño L., Kafarov V., Saavedra J., 2013, Effect of the composition of the refinery gas on the characteristics of the combustion process, *Engineering Journal University of Medellín*, 12, 101-111.
- Casallas Q., 2011, Corrosion and Industrial Maintenance, *Free Wit Journal*, 10, 29-32.
- Galerie A., Petit J., Wouters Y., Mougín J., Srisual A., Hou P., 2011, Water vapour effects on the oxidation of chromia-forming alloys, *Materials Science Forum*, 696, 200-205.
- Gamo R., 2016, coatings resistant to the degradation phenomena in the new steam turbines, PhD Thesis, Complutense University of Madrid, Madrid, Spain.
- Kafarov V., Toledo M., Meriño L., 2015, Numerical simulation of combustion process of fuel gas mixtures at refining industry, *Chemical Engineering Transactions*, 43, 1351–1356.
- Asrar N., MacKay B., Birketveit O., Stipaničev M., Jackson J., Jenkis A., Melot D., Scheie J., Vittonato J., 2016, Corrosion: The most extensive struggle, *Oilfield Review*, 28, 36–50.
- Peña D., Estupiñan E., Nava J., Infanzon D., Alvarez A., 2014, High Temperature Oxidation of ASTM A335 P 92 steel in Isothermal and Thermal Cycling Conditions, *Fuentes The Energy Rebound Journal*, 12, 5-13.
- Peña D., Vásquez C., Laverde D., Serna A., 2012, Corrosion at high temperature of 9Cr-1Mo modified P91 ferritic steel, in simulated oxidant-fuel atmospheres, *Journal of Metallurgy*, 48, 97–106.
- Pettit F., 2011, Hot Corrosion of Metals and Alloys, *Oxidation of Metals*, 76, 1–21.
- Saavedra J., Merino L., Gómez M., Kafarov V., 2014, Combustion Optimisation using Methane Number and Wobbe Index as Evaluation Criteria, 39, 1231–1236.
- Young D. (Ed), 2016, High Temperature Oxidation and Corrosion of Metals, Elsevier Corrosion Series, Cambridge, UK.